

RD-R48 125

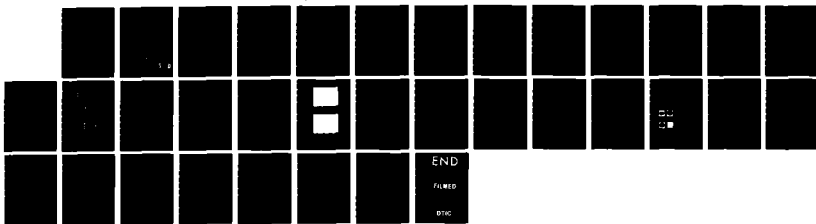
LONG PULSE E-BEAM CONTROLLED SWITCH: DESCRIPTION OF  
APPARATUS AND INITIAL RESULTS (U) NAVAL RESEARCH LAB  
WASHINGTON DC J BURTON ET AL. 30 AUG 85 NRL-MR-5628

1/1

UNCLASSIFIED

F/G 9/5

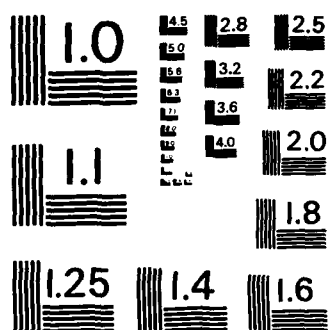
NL



END

FILMED

BTM



MICROCOPY RESOLUTION TEST CHART  
NATIONAL BUREAU OF STANDARDS - 1963 - A

## Long Pulse E-Beam Controlled Switch: Description of Apparatus and Initial Results

J. BURTON,\* V. E. SCHERRER, R. J. COMMISSO  
R. F. FERNSLER AND I. M. VITKOVITSKY

*Plasma Technology Branch  
Plasma Physics Division*

*\*Sachs/Freeman Associates, Inc.  
Bowie, MD 20715*

AD-A159 125

August 30, 1985

This work was supported by the Office of Naval Research, the Naval Sea Systems Command,  
and the Naval Surface Weapons Center.



NAVAL RESEARCH LABORATORY  
Washington, D.C.

*S DTIC  
SEP 11 1985  
A*

Approved for public release; distribution unlimited.

85 9 10 145

DTIC FILE COPY

SECURITY CLASSIFICATION OF THIS PAGE

AD-A159 125

## REPORT DOCUMENTATION PAGE

1a REPORT SECURITY CLASSIFICATION <b>UNCLASSIFIED</b>		1b RESTRICTIVE MARKINGS													
2a SECURITY CLASSIFICATION AUTHORITY		3 DISTRIBUTION / AVAILABILITY OF REPORT <b>Approved for public release; distribution unlimited.</b>													
2b DECLASSIFICATION / DOWNGRADING SCHEDULE															
4 PERFORMING ORGANIZATION REPORT NUMBER(S) <b>NRL Memorandum Report 5628</b>		5. MONITORING ORGANIZATION REPORT NUMBER(S)													
6a NAME OF PERFORMING ORGANIZATION <b>Naval Research Laboratory</b>	6b OFFICE SYMBOL (If applicable) <b>Code 4770</b>	7a. NAME OF MONITORING ORGANIZATION													
6c ADDRESS (City, State, and ZIP Code) <b>Washington, DC 20375-5000</b>		7b. ADDRESS (City, State, and ZIP Code)													
8a. NAME OF FUNDING / SPONSORING ORGANIZATION <b>ONR, NAVSEA and NSWC</b>	8b. OFFICE SYMBOL (If applicable)	9. PROCUREMENT INSTRUMENT IDENTIFICATION NUMBER													
8c. ADDRESS (City, State, and ZIP Code) <b>Arlington, VA 22217</b> <b>Washington, DC 20362</b>		10. SOURCE OF FUNDING NUMBERS <table border="1"><tr><td>PROGRAM ELEMENT NO (See page ii)</td><td>PROJECT NO</td><td>TASK NO.</td><td>WORK UNIT ACCESSION NO.</td></tr></table>		PROGRAM ELEMENT NO (See page ii)	PROJECT NO	TASK NO.	WORK UNIT ACCESSION NO.								
PROGRAM ELEMENT NO (See page ii)	PROJECT NO	TASK NO.	WORK UNIT ACCESSION NO.												
11. TITLE (Include Security Classification) <b>Long Pulse E-Beam Controlled Switch: Description of Apparatus and Initial Results</b>															
12. PERSONAL AUTHOR(S) <b>Burton, J., * Scherrer, V.E., Comisso, R.J., Fernsler, R.F. and Vitkovitsky, I.M.</b>															
13a. TYPE OF REPORT <b>Interim</b>	13b. TIME COVERED FROM _____ TO _____	14. DATE OF REPORT (Year, Month, Day) <b>1985 August 30</b>	15. PAGE COUNT <b>34</b>												
16. SUPPLEMENTARY NOTATION <b>*Sachs/Freeman Associates, Inc., Bowie, MD 20715</b> (Continues)															
17. COSATI CODES <table border="1"><tr><th>FIELD</th><th>GROUP</th><th>SUB-GROUP</th></tr><tr><td> </td><td> </td><td> </td></tr><tr><td> </td><td> </td><td> </td></tr><tr><td> </td><td> </td><td> </td></tr></table>		FIELD	GROUP	SUB-GROUP										18. SUBJECT TERMS (Continue on reverse if necessary and identify by block number) <b>Fast opening switches ; Inductive storage ; Repetitive opening switches ; Diffuse discharge .</b>	
FIELD	GROUP	SUB-GROUP													
19. ABSTRACT (Continue on reverse if necessary and identify by block number) <b>The design of an inductive store system that employs an electron-beam controlled switch to produce a 280 kV, 10 kA, 60 ns full width at half maximum pulse is described. Included in the design are the electron-beam generator, electron-beam diode, and electron-beam controlled switch. The voltage is generated across an open circuit load. These non-optimized results agree with predictions from a previously described design procedure.</b>															
20. DISTRIBUTION / AVAILABILITY OF ABSTRACT <input checked="" type="checkbox"/> UNCLASSIFIED/UNLIMITED <input type="checkbox"/> SAME AS RPT <input type="checkbox"/> DTIC USERS		21. ABSTRACT SECURITY CLASSIFICATION <b>UNCLASSIFIED</b>													
22a. NAME OF RESPONSIBLE INDIVIDUAL <b>R. J. Comisso</b>		22b. TELEPHONE (Include Area Code) <b>(202) 767-2468</b>	22c. OFFICE SYMBOL <b>Code 4770</b>												

DD FORM 1473, 84 MAR

83 APR edition may be used until exhausted  
All other editions are obsolete

SECURITY CLASSIFICATION OF THIS PAGE

SECURITY CLASSIFICATION OF THIS PAGE

**10. SOURCE OF FUNDING NUMBERS**

PROGRAM ELEMENT NO.	PROJECT NO.	TASK NO.	WORK UNIT ACCESSION NO.
61153N	RR011-09-41		DN320-105
62768N	SF6P-345-001		DN080-273

**16. SUPPLEMENTARY NOTATION (Continued)**

This work was supported by the Office of Naval Research, the Naval Sea Systems Command, and the Naval Surface Weapons Center.

SECURITY CLASSIFICATION OF THIS PAGE

## CONTENTS

I. INTRODUCTION .....	1
II. E-BEAM GENERATOR .....	3
A. High Voltage Generator .....	5
B. Output Switch .....	8
C. Divert Switch .....	8
D. Divert Switch Trigger Circuit .....	8
E. System Test .....	12
III. E-BEAM DIODE .....	15
A. Diode Design .....	15
B. Diode Electrical Characteristics .....	16
C. E-Beam Uniformity .....	19
IV. EBCS - DESIGN AND INITIAL RESULTS .....	19
A. Experimental Setup .....	19
B. Initial Results .....	24
V. PROPOSAL FOR FUTURE WORK .....	27
ACKNOWLEDGMENTS .....	28
REFERENCES .....	29

## LONG PULSE E-BEAM CONTROLLED SWITCH: DESCRIPTION OF APPARATUS AND INITIAL RESULTS

### I. INTRODUCTION

There exists an interest in the application of externally controlled high pressure, volume discharges to high power switching. The applications of particular importance involve opening switches for both single and repetitively pulsed, high power, inductive generators.<sup>1</sup> Such discharges have great potential for these applications because they can recover rapidly to the original highly resistive state of the gas once the external ionizing agent is removed.

Several authors<sup>2-9</sup> have reported on experiments and theoretical investigations in which an electron beam (e-beam) is used as the external agent to sustain the diffuse discharge. The concept as it might be used in an opening switch application is illustrated in Fig. 1. The accelerated e-beam is injected through a thin foil (that serves as a vacuum interface) into a chamber filled with a non-attaching base gas along with a small admixture (~ 1%) of an attaching gas at a pressure of 1 - 10 atm. The gas resistivity at any time is determined by a competition between ionization provided by the e-beam and the various recombination and attaching processes characteristic of the specific gas mixture, pressure, and applied electric field. This, along with the volume discharge property, allows the gas to return to its original nonconducting state very quickly once the source of ionization is removed. The particular advantages of this switching scheme are: 1) the intrinsic switching can be made very fast<sup>7</sup> (~ 1 ns), 2) there is a potential for repetitive operation at > 10 kHz in a burst mode,<sup>7</sup> and 3) the

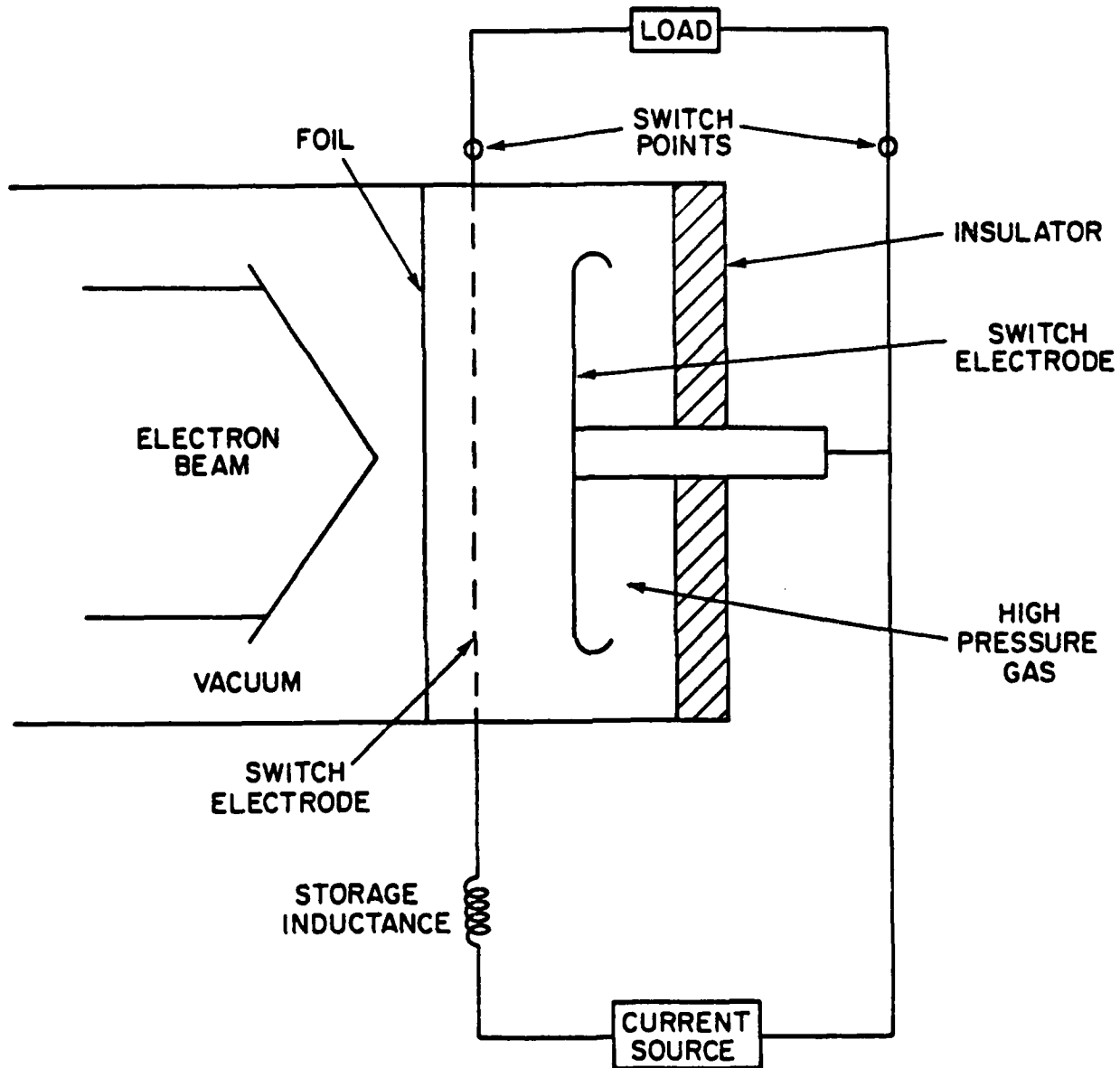


Fig. 1. Illustration of an opening switch application for an e-beam controlled diffuse discharge.

switch inductance, mechanical shock, and electrode wear can be minimized because of the diffuse nature of the discharge.

Most of the work with e-beam controlled switches (EBCS) has been done at either low switch currents ( $\sim$  mA) or short switch conduction times ( $\sim$  100 ns). In this report we describe the design of a system for studying the switch behavior in the  $\approx$  1  $\mu$ s conduction time regime and at a switch current of  $\approx$  10 kA. Figure 2 is a drawing of the entire system illustrating the relative positions of the components. Section II contains a detailed description of the circuitry and triggering for the e-beam generator. The generator produces several kiloamps of e-beam current at  $\approx$  300 kV for variable pulse lengths of 0.5 - 5.0  $\mu$ s. The e-beam diode and experiments aimed at characterizing the diode and e-beam behavior are described in Sec. III. Design of the e-beam controlled switch (EBCS) along with results from initial switching experiments are discussed in Sec. IV. The EBCS, operated with 1%  $C_2F_6$  and 99%  $CH_4$  conducted current provided by a capacitor (originally charged to  $\approx$  26 kV) for  $\approx$  0.7  $\mu$ s while energizing an  $\approx$  1.5  $\mu$ H inductor. It then opened on command at a current of  $\approx$  10 kA, generating a voltage pulse of  $\approx$  280-kV amplitude and  $\approx$  60- ns full width at half maximum (FWHM). This was accomplished with an open circuit load. In Sec. V we make suggestions for future work.

## II. E-Beam Generator

To provide a power source for extending the conduction time of the EBCS to  $\approx$  1  $\mu$ s, a variety of power supplies to drive a vacuum e-beam diode were considered. The requirements were determined from a self-consistent design procedure<sup>1</sup>. The diode needed to provide 300 kV for up to 1.5  $\mu$ sec at a current of 1 kA. The generator had to be constructed with no new major

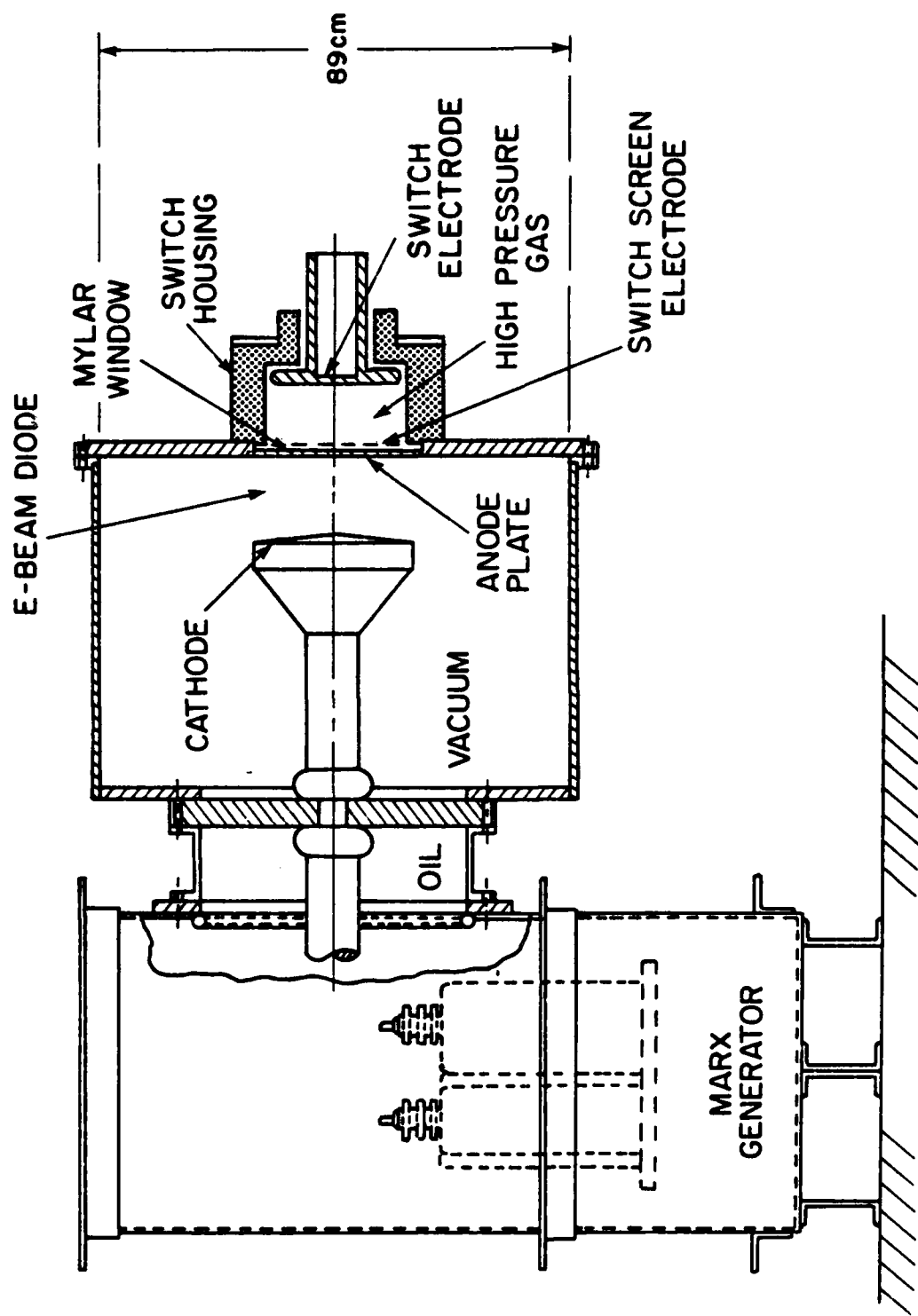


Fig. 2. Illustration of EBCS system components.

procurement. The diode required a cathode area of  $\sim 700 \text{ cm}^2$  and an anode-cathode (AK) gap adjustable from 5 to 15 cm. The voltage on the diode was applied as a pulse with a rise time not exceeding 0.2  $\mu\text{sec}$  and a decay time no longer than 0.07  $\mu\text{sec}$ . The droop of the pulse is determined by the stored energy and this in turn was determined by cost and space limitations.

Taking all of the above requirements into account, a variety of potential generators for driving such a diode were analyzed using the BERTHA<sup>10</sup> code. This study resulted in the decision to build a Marx type generator consisting of six stages of 0.5- $\mu\text{F}$ , 50-kV capacitors. The results of the modeling for such a generator driving an e-beam diode assuming a closure speed of 2  $\text{cm}/\mu\text{s}$  were obtained. The voltage and current from these results for indicated times after the start of current flow in the diode are compared for three initial AK spacings in Table I.

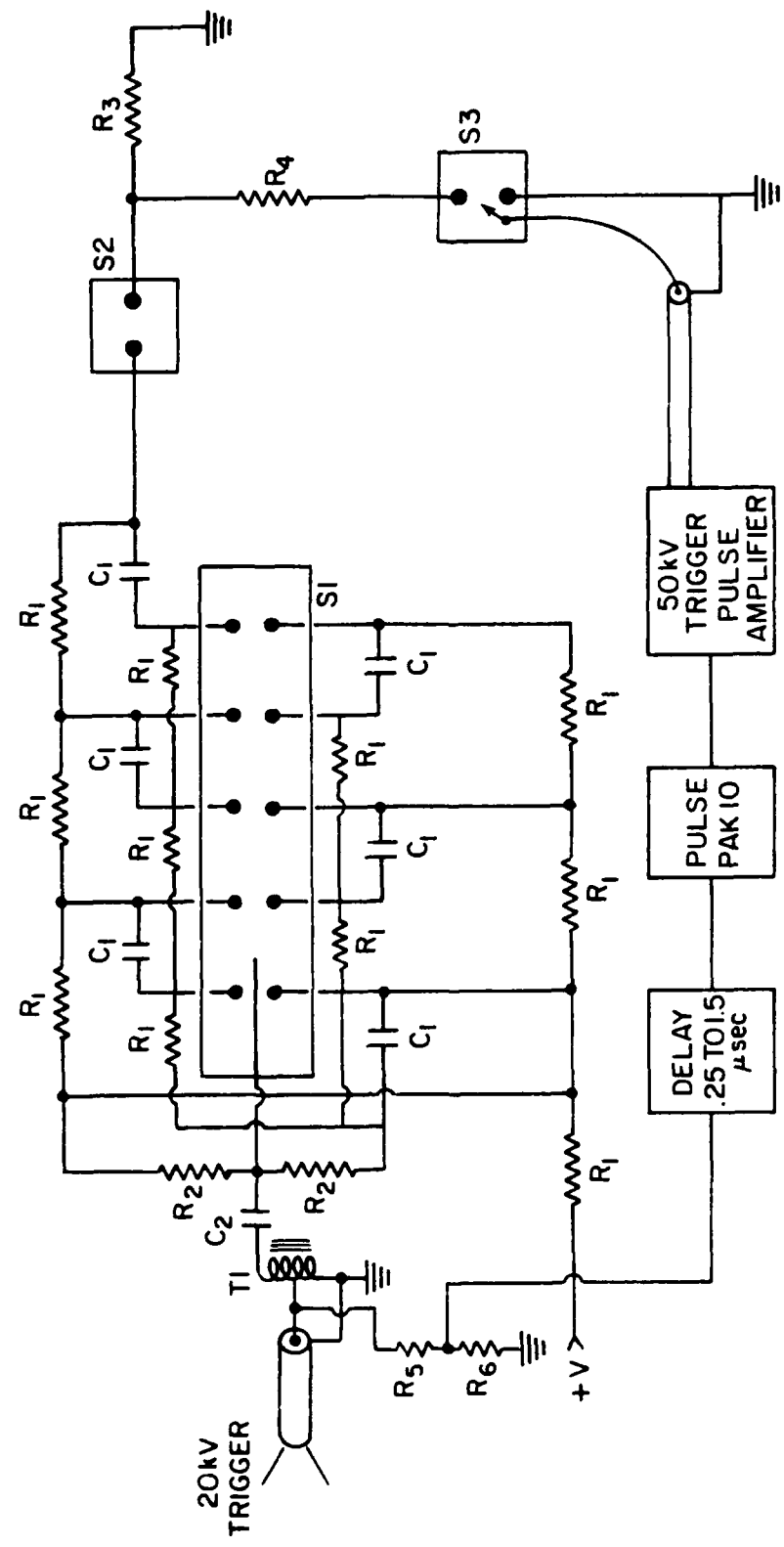
#### A. High Voltage Generator

A six stage oil insulated generator using an  $n = 2$  Marx configuration was selected for the pulse generator. The Marx circuit diagram, along with a schematic layout of the triggering system is shown in Fig. 3. To simplify triggering and provide fast, low jitter erection a switch column having a single trigger electrode rather than individual triggered switches was used. It has been our experience that the beneficial effects of the uv illumination obtained from the switch column clearly outweigh any maintenance problems when used on a small, 5 or 6 stage machine. The use of a column with single stage triggering also reduces the complexity of the trigger generator. To assure reliable triggering and permit the use of some existing components, a 5:1 step-up transformer was used to boost the output of the available standard 20-kV trigger pulse amplifier (TPA) to 100 kV.

Converting the conventional Marx output to one with an adjustable width, rectangular pulse was accomplished by adding two switches -- the first switch (S-2 of Fig. 3) provided an untriggered Marx output and the second switch (S-3 of Fig. 3) provided the divert function to control (clip) the length of the pulse.

Table I - Marx Voltage ( $V_m$ )  
 and Marx Current ( $I_m$ ) Produced by a Six Stage  
 Marx Pulse Generator (.5  $\mu$ F/Stage)

Time after current initiation ( $\mu$ s)	<u>0.5</u>	<u>1.0</u>	<u>1.5</u>	<u>2.0</u>
$V_m$ (kV)	279	270	266	261
AK = 14 cm				
$I_m$ (A)	660	647	737	848
$V_m$ (kV)	272	267	261	254
AK = 12 cm				
$I_m$ (A)	827	878	1020	1200
$V_m$ (kV)	271	262	253	242
AK = 10				
$I_m$ (A)	1190	1250	1490	1800



$R_1$  - 3000 OHM SOLUTION RESISTOR  
 $R_2$  - 10 M OHM MATCHED  
 $R_3$  - "DIODE"  
 $R_4$  - 0.6 OHM  
 $R_5$  - 50,000 OHM  
 $R_6$  - 50 OHM  
 $C_1$  - .5 $\mu$ F 50kV  
 $C_2$  - 800 pF 120kV  
 S1 - SWITCH COLUMN  
 S2 - SELF CLOSING OUTPUT SWITCH  
 S3 - TRIGATRON DIVERT SWITCH  
 T1 - TRANSFORMER SWITCH 5:1

Fig. 3. Circuit diagram of Marx and schematic layout of triggering system.

### B. Output Switch

To provide the fast risetime (0.2  $\mu$ sec) of the voltage pulse applied to the e-beam diode a simple two-electrode, gas-insulated switch was used (S-2 of Fig. 3). Depending on the insulating gas, this switch is useful to over 500 kV when operated in a pulse charged system. This is illustrated in Fig. 4, which is a plot of the self-breakdown voltage of the output switch as a function of the switch gas pressure for various gas mixtures. Since the switch has an overall body length of only six inches it must be operated in an insulating medium such as oil or water.

### C. Divert Switch

This switch has the requirements of: 1) withstanding a 300 kV pulse, 2) being triggered satisfactorily by the 50-kV TPA that was available, and 3) having low jitter. The trigatron type switch, when operated at greater than 80% of its self-break voltage has very low jitter. In addition, the trigger circuit for this type switch is operated at ground potential. To meet the voltage requirements, a trigatron that was developed some years earlier<sup>11</sup> for 100 kV DC service was modified and used. A drawing of this switch is shown in Fig. 5. The necessary modification was to increase the switch body length by 1.25 cm so that the electrode gap would increase from 1.65 cm to 2.9 cm. The self-breakdown voltage was then measured as a function of pressure up to 300 kV as shown in Fig. 6, using as an insulating gas a mixture of 90% N<sub>2</sub> with 10% SF<sub>6</sub>.

### D. Divert Switch Trigger Circuit

A timing signal to trigger the divert switch (S-3 of Fig. 3) must be taken from the Marx circuit at a point that permits the overall jitter of the

in ~ 70% transmitting brass screen anode and a 25-cm diam aluminum cathode. The AK spacing could be adjusted from 0 - 20 cm. The anode plate for the e-beam diode was drilled with 0.47-cm diam holes within a 25-cm diam such that the fraction of open area was 0.68. A  $5 \times 10^{-3}$ -cm thick (2 mil) mylar sheet served as the vacuum-switch interface. The energy loss of a 250-keV electron in the mylar is  $\approx$  18 keV. The e-beam current in the switch,  $I_b$ , was measured with a Rogowski coil (see Fig. 13).

The switch housing was fabricated from cast plastic. The entire switch was designed to be pressurized to  $\leq$  20 atm. Originally the switch was surrounded by air. However, because of the high voltage generated, the switch was eventually submerged in oil.

Diagnostics used included calibrated Rogowski coils, magnetic probes, and a calibrated voltage divider. An attempt was made to calibrate the Rogowski coils against a known monitor at frequencies comparable with the fastest observed in the experiment. The Rogowski coils (one commercial and one homemade) showed signs of poor response for the signals with characteristic risetimes of  $\leq$  15 ns. The problem associated with this diagnostic is the difficulty in building a loop of sufficient sensitivity to the slowly varying part of the current, yet with low enough inductance to follow the rapidly varying part of the current as well. Because of limitations on laboratory time resulting from budget constraints, the magnetic probes could not be successfully implemented.

The switch dimensions, gas mixture, gas pressure, and e-beam generator requirements were all self-consistently determined using the design procedure described in Ref. 1. This technique combines the switch physics with the desired switching performance to analytically estimate the switch area, length, gas mixture and pressure, and the e-beam generator requirements.

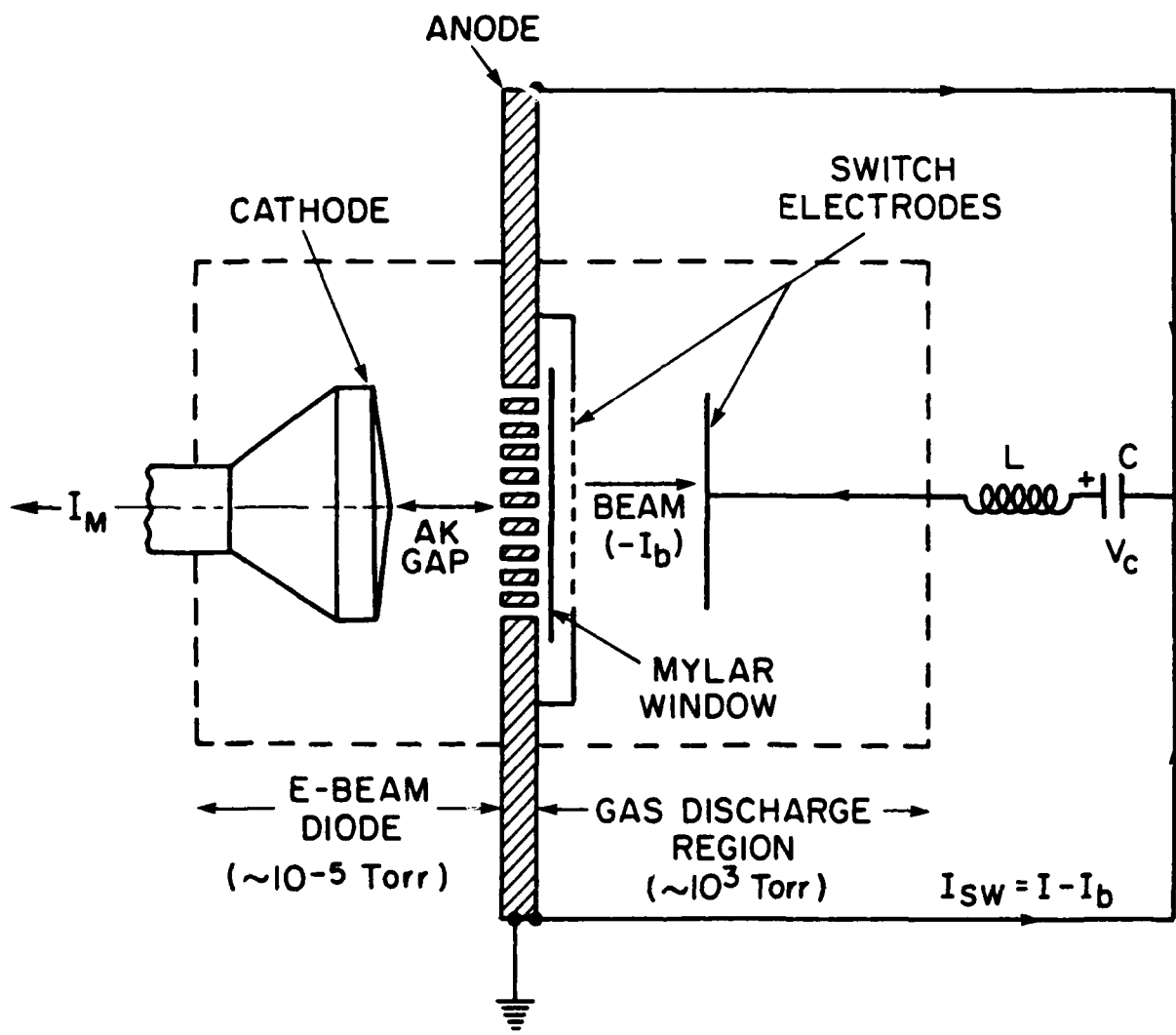


Fig. 12. Schematic depiction of EBCS and associated circuit.

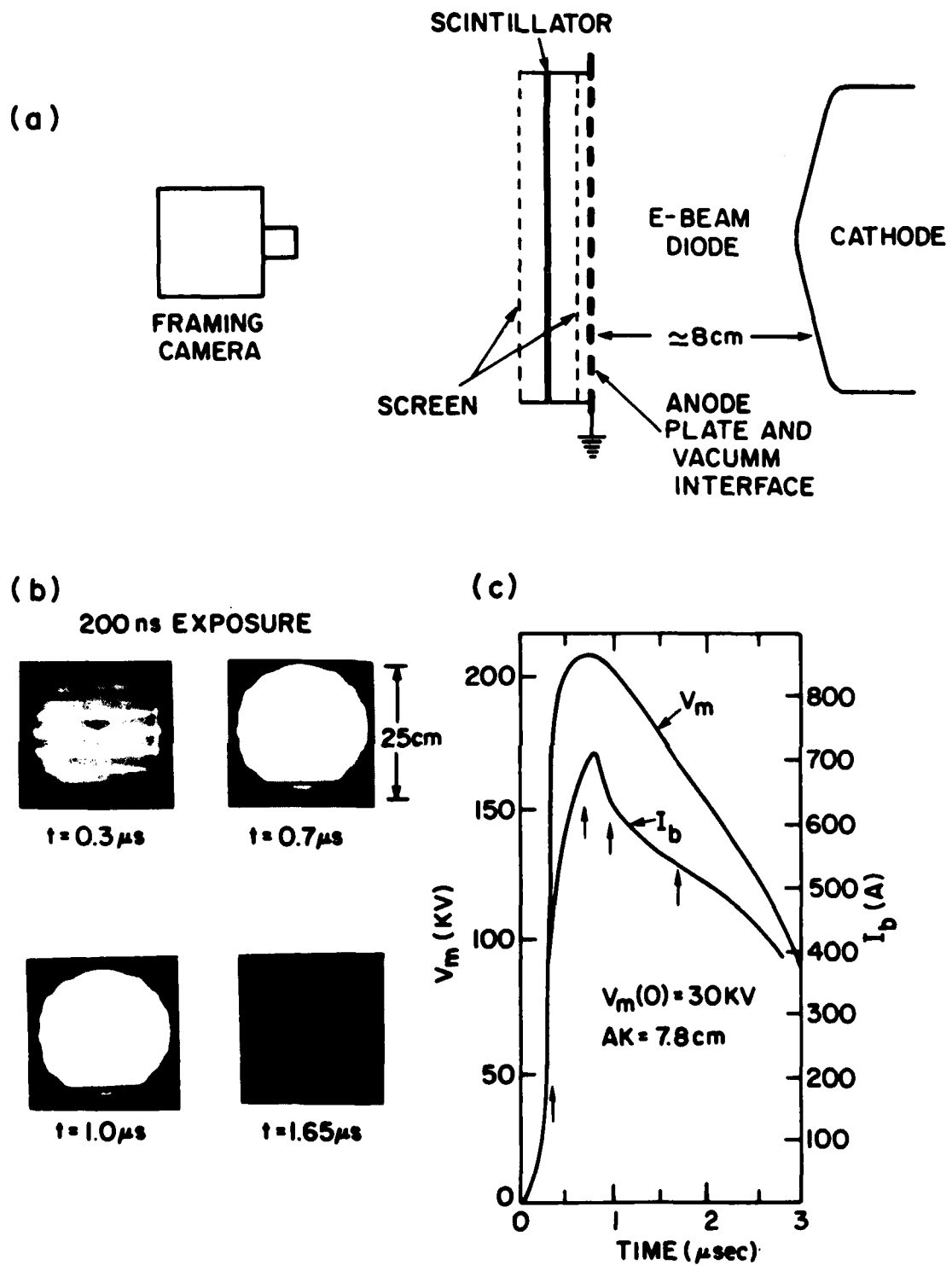


Fig. 11. Illustration of e-beam uniformity measurements: (a) Schematic showing relative positions of framing camera, scintillator, anode plate and e-beam diode; (b) typical data taken with framing camera; (c) Marx voltage,  $V_m$ , and e-beam current,  $I_b$ , incident on scintillator, as functions of time. Arrows indicate times at which framing camera exposures were made.

at  $t \approx 0.6 \mu s$  is a result of the oscillation in  $V_m$  at that time. A likely cause for this oscillation may be the ringing frequency of the Marx capacitance and diode inductance through the diode stray capacitance to ground.

We assumed the radial electric field associated with the beam is effectively shorted at the anode surface so that beam expansion was considered to be an unimportant effect. This will be the case to the extent that the cathode diameter (30.5 cm) is much larger than the AK gap spacing ( $\leq 10$  cm for the work reported here).

### C. E-Beam Uniformity

The uniformity of the electron beam entering the switch region (see Fig. 2) was studied as illustrated in Fig. 11. The light generated from the e-beam incident on a 25 cm-diam, 0.16-cm thick (62 mills) piece of NE 102A plastic scintillator (2.4-ns decay time) was photographed using a fast framing camera. The range of a 250-keV electron in plastic is  $\approx 0.08$  cm.

As can be seen from the data [Fig. 11(b)], the beam is fairly uniform (the dark horizontal lines are an artifact associated with the camera). The light intensity on the scintillator will depend on the power deposited by the electrons, i.e., on both  $V_m$  and  $I_b$ . The film/camera sensitivity was not determined.

## IV. EBCS - Design and Initial Results

### A. Experimental Setup

A schematic representation of the EBCS and associated circuit is shown in Fig. 12. The switch hardware is illustrated in Fig. 13. It consists of

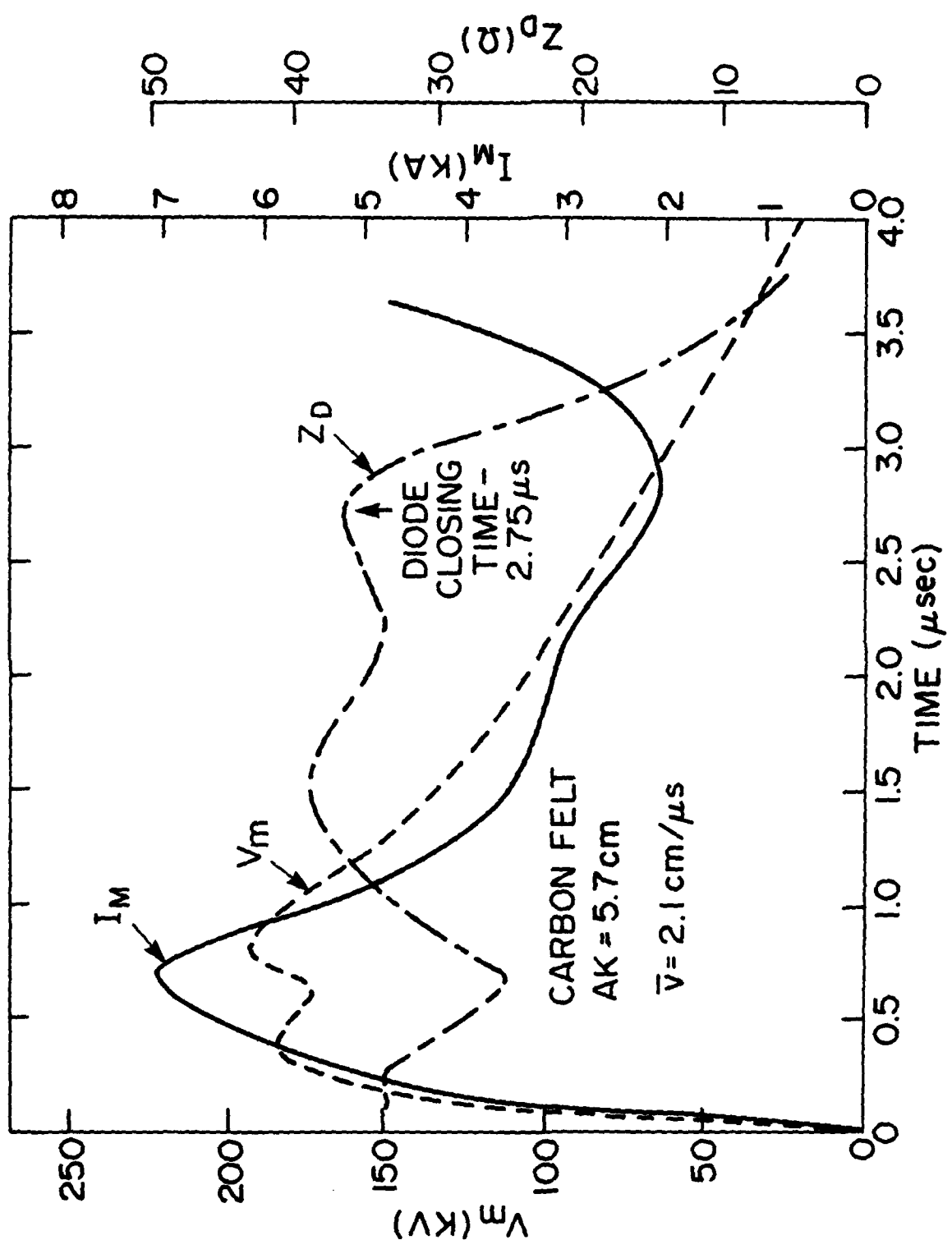


Fig. 10. Diode electrical characteristics. Here the cathode material is carbon felt and the  $AK$  spacing is  $5.7 \text{ cm}$ .

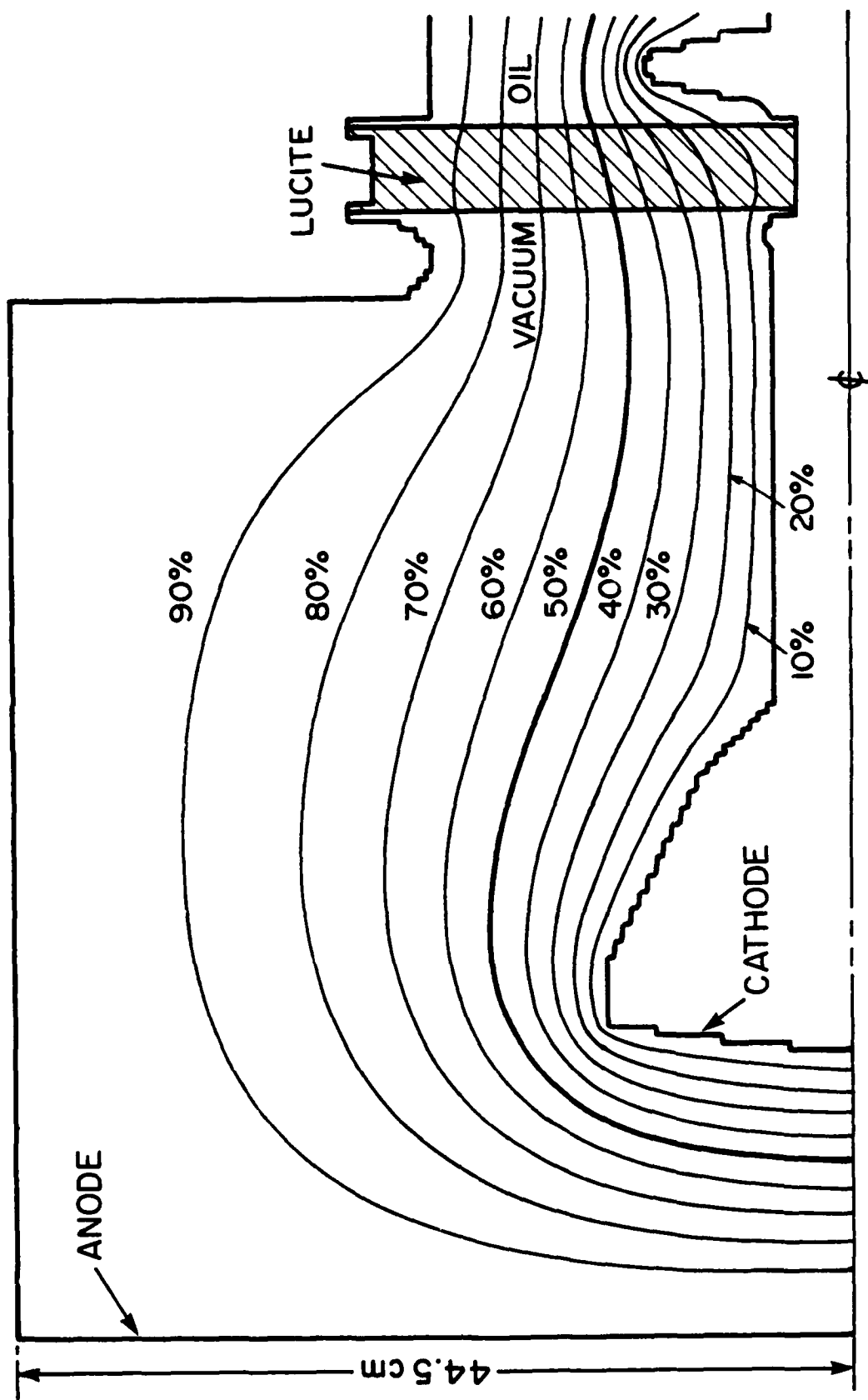


Fig. 9. Plot of equipotentials in the diode region in percent of total potential difference between anode and cathode.

This situation could be improved by shaping the cathode shank on the vacuum side of the lucite insulator.

Carbon felt was chosen as the cathode material. This choice was made to minimize the AK gap plasma closure velocity and for potential repetitive pulse work.<sup>13</sup>

#### B. Diode Electrical Characteristics

The Marx current,  $I_m$ , and voltage,  $V_m$ , are plotted in Fig. 10 as a function of time for an AK gap of 5.7 cm. With AK gaps greater than this, no obvious diode closure was observed during the pulse. The initial Marx charging voltage was  $V_m(0) = 30$  kV. Also shown is the calculated diode impedance  $Z_D = V_D/I_D \approx V_m/I_m$ , where  $V_C$  and  $I_D$  are the voltage across and current through the diode, respectively. Note that  $V_m$  was measured using a calibrated resistive voltage divider on the oil side of the lucite vacuum/oil interface, (see Figs. 9 and 2) so that the diode voltage  $V_D = V_m - L_D dI_m/dt$ , where  $L_D$  is the inductance between the voltage divider and the diode. For this system  $L_D \leq 200$  nH and from Fig. 10  $dI_m/dt \leq 2 \times 10^{10}$  A. Thus, during the time of interest, the correction term,  $L_D dI_m/dt$ , is small ( $\leq 4$  kV) compared with  $V_m$  ( $\approx 200$  kV) and has been neglected, i.e.,  $V_D \approx V_m$ . Also, we assumed  $I_D = I_m$  where  $I_D$  is the diode current. Note, the e-beam current that actually enters the switch is  $< I_D$  as a result of attenuation through the anode plate/vacuum window structure (see Figs. 1 and 2).

The diode impedance calculated in this way is  $25 \Omega \leq Z_D \leq 35 \Omega$  between  $t = 0.8$  and  $t = 2.5 \mu s$ , where  $t$  is the time measured from the diode voltage initiation. At  $t = 2.75 \mu s$ ,  $Z_D$  begins to decrease sharply. Chosing this as time at which the electrode plasma closes the AK gap gives an average AK gap closure speed of  $\bar{v} \approx 2.1$  cm/ $\mu s$ . The small relative decrease in  $Z_D$

the self-closing output switch does show some jitter. This has been improved by providing a small gas flow in the output switch rather than the static pressurizing system used in this test. The maximum controlled pulse width is determined by the voltage decay across the divert switch because once below a minimum voltage the switch will not fire.

### III. E-Beam Diode

#### A. Diode Design

The diode is directly connected to the Marx generator as shown in Fig. 2. It has a rather large emitting surface area ( $730 \text{ cm}^2$ ) and has the requirement that the AK gap be variable from 5 cm to 15 cm. The diode chamber is relatively large to minimize emission to areas other than the anode. To help in this and other diode design problems an electrostatic field plotting code<sup>12</sup> was used to optimize the three critical areas of diode designs: the shape of the front surface of the cathode, minimizing emission to areas other than to the anode, and the field grading of the lucite insulator between the oil in the Marx generator and the diode vacuum. The overall field plot of the diode is shown in Fig. 7. The first two of the three objectives were achieved but in doing so the third - that of optimizing the field grading on the lucite insulator - was only partially achieved. As can be seen from the field plot the grading of voltage across the vacuum-lucite interface is reasonably uniform across the surface but in doing this the angle the field lines make with the insulator surface is close to  $90^\circ$ . This condition is not optimum for suppressing electron multiplication or other types of streamer growth and is only acceptable in this case because of the relatively low voltage involved.

WITHOUT DIVERT SWITCH

(a)

200 KV

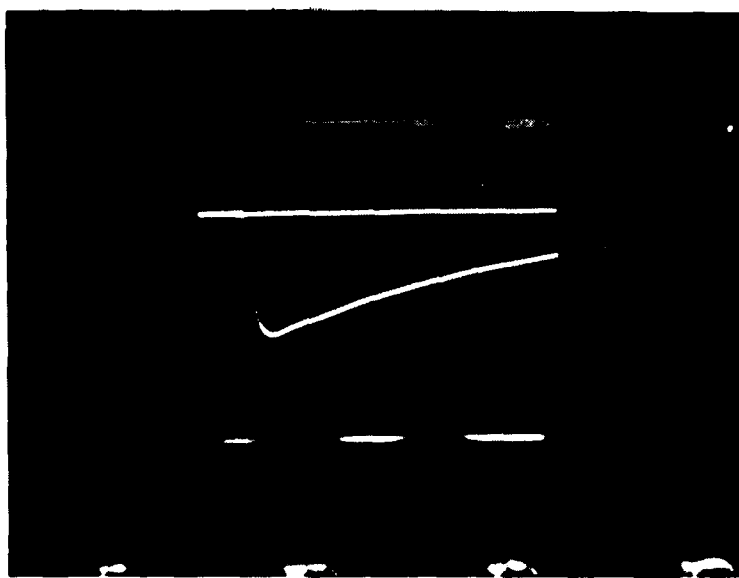


OUTPUT VOLTAGE  
0.5 $\mu$ s/DIV

WITH DIVERT SWITCH

(b)

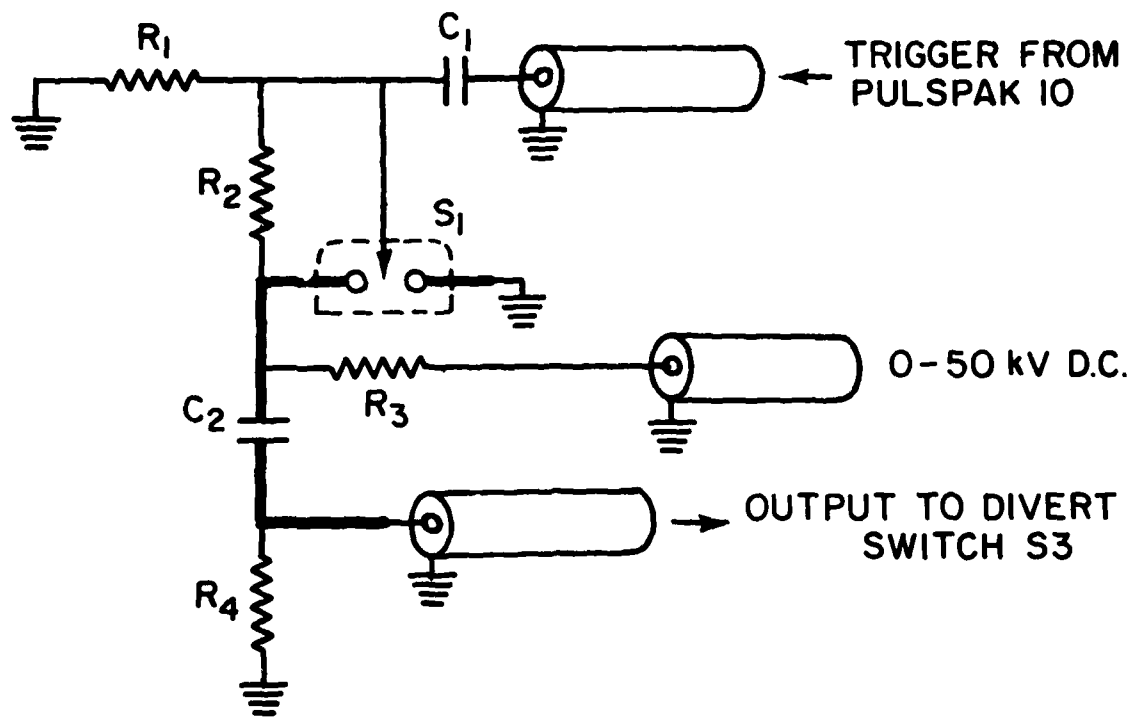
200 KV



OUTPUT VOLTAGE  
0.2 $\mu$ s/DIV

Fig. 8. (a) Output voltage of e-beam generator into a  $100 \Omega$  dummy load with no divert switch. (b) Output voltage of e-beam generator into a  $100 \Omega$  dummy load with divert switch set to minimum pulse width.

## 50 kV TRIGGER PULSE AMPLIFIER



$R_1, R_2$  - 100 Meg OHMS

$R_3$  - 10 Meg OHMS

$R_4$  - 100 OHMS

$C_1$  -  $2.5 \mu\text{F}$ , 40 kV

$C_2$  -  $.05 \mu\text{F}$  50 kV [HIGH ENERGY # ML101]

$S_1$  - SW 50K

HEAVY LINE DENOTES MINIMUM INDUCTANCE WIRING

Fig. 7. Circuit diagram of 50 kV TPA for triggering the divert switch.

divert system to be less than 10% of the minimum output pulse width. Fortunately the Marx erection circuit exhibits very low jitter so that a signal can be taken from the output of the 20 kV TPA triggering the Marx. Picking up the trigger signal this early in the Marx erection time increases the minimum internal delay required of the divert switch triggering circuit. The timing signal is then passed through a standard low level delay generator after which it must be amplified to the 50 kV level to provide the divert switch trigger. The first stage in this amplification is the Pulspak 10 -- a commercial generator (Physics International Company) that operates from a 10-V input signal to provide a 10-kV output pulse into  $50\ \Omega$  with a throughput delay of 70 ns and a shot-to-shot jitter of  $\pm 1$  ns. The Pulspak output is used to trigger a 50-kV TPA, illustrated in Fig. 7, that was designed for this task. This TPA, when driven by the Pulspak, increases the throughput delay to 80 ns and does not measurably change the shot-to-shot jitter of  $\pm 1$  ns. The total delay of the divert switching circuit is, neglecting cable delays, less than 100 ns and the overall jitter including the Marx generator is less than  $\pm 10$  ns.

#### E. System Test

The Marx, with the output switch and the adjustable delayed divert switch, was operated with a  $100-\Omega$  resistive load in place of the diode to check system operation. The system was first operated with the output switch installed but without the divert circuit functioning. A typical waveform for this is shown in Fig. 8(a). Next, the divert circuit was operated providing the minimum width output pulse shown in Fig. 8(b). Displayed in Fig. 8(b) is a five shot exposure showing that, at the oscilloscope sweep speed chosen (0.2  $\mu$ s /div), there was no measurable jitter of the fall of the pulse while

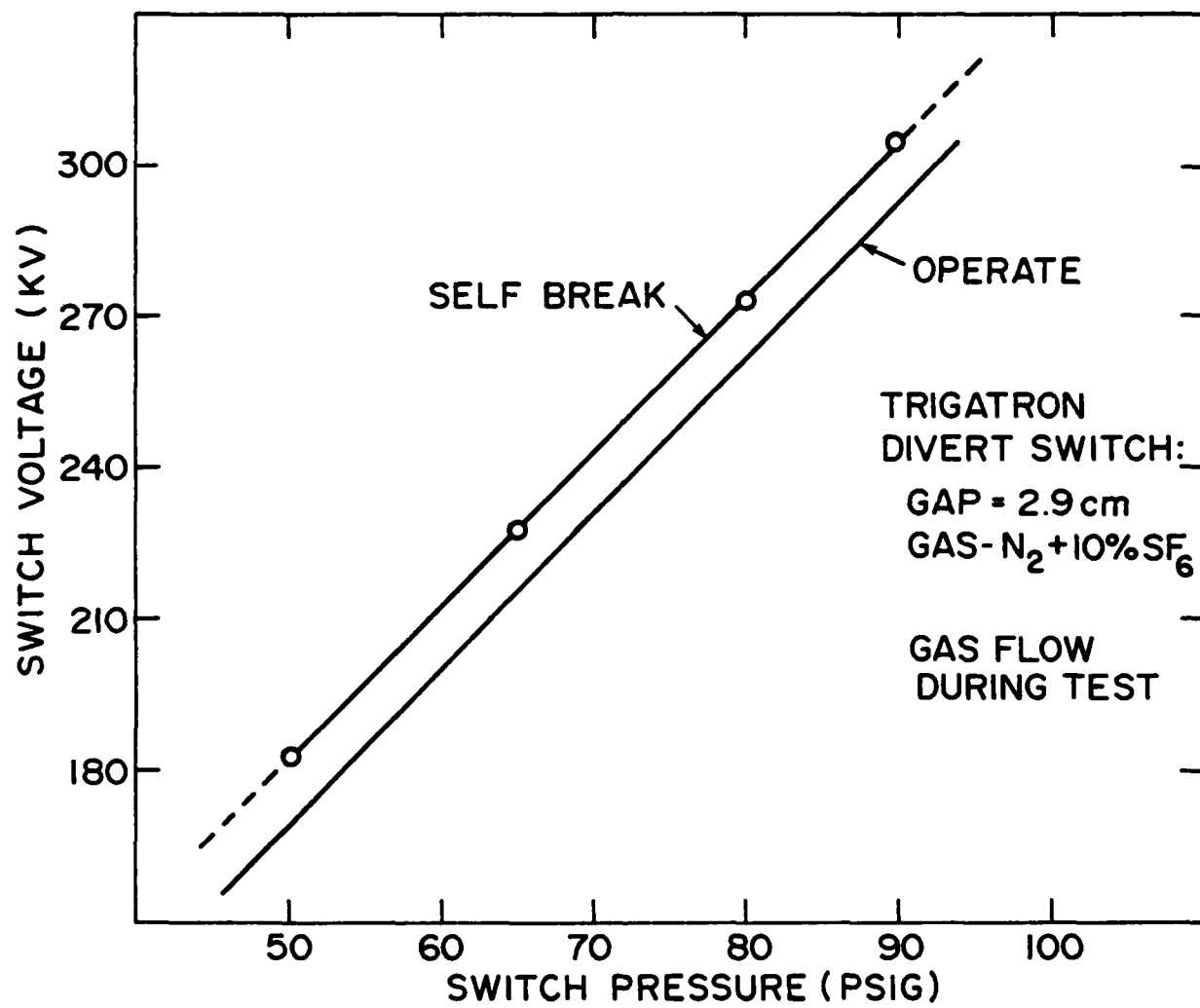


Fig. 6. Plot of self-breakdown voltage of the divert switch (S-3 in Fig. 3) as a function of switch pressure. A small gas flow was maintained through the switch.

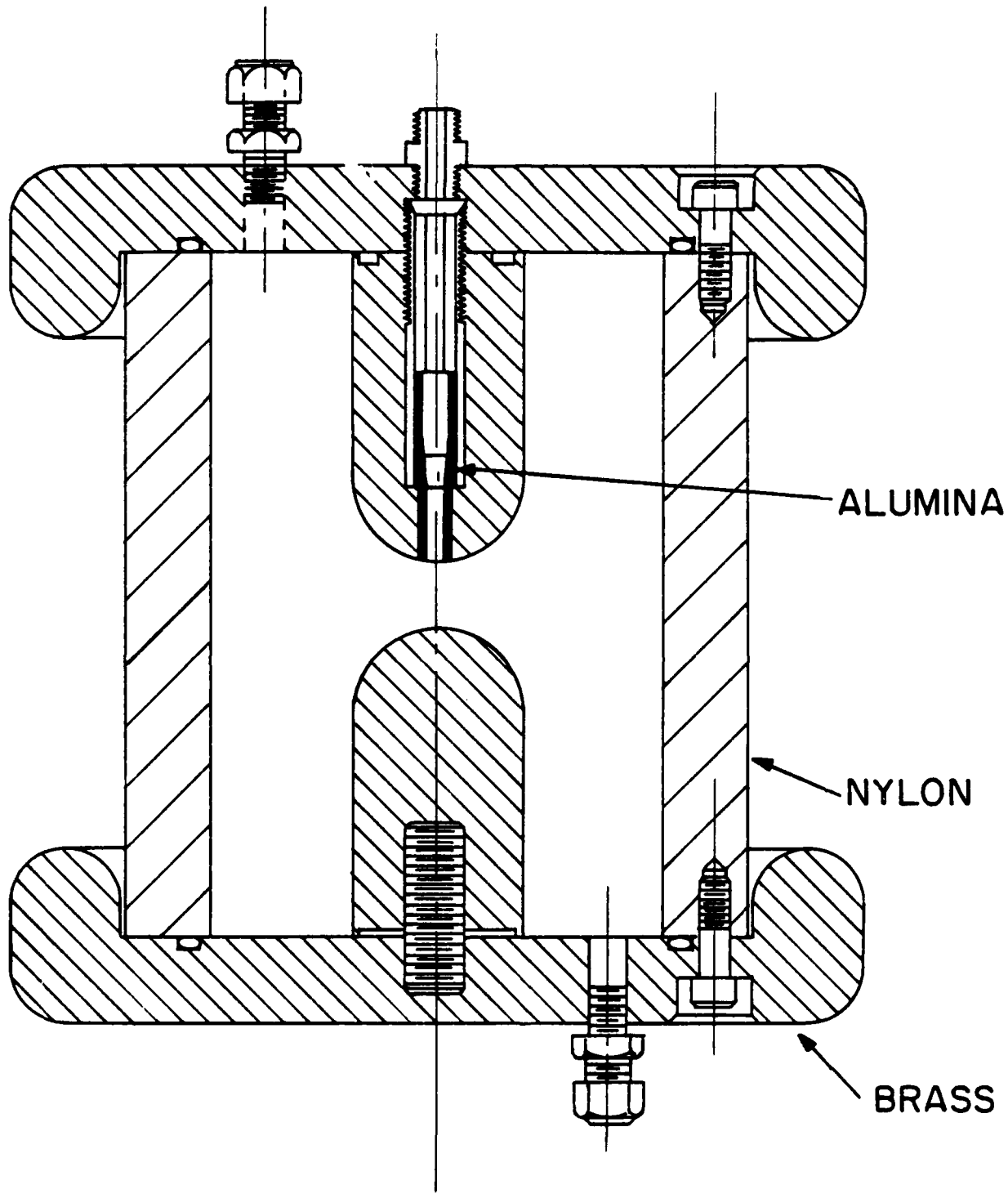


Fig. 5. Schematic drawing of divert switch.

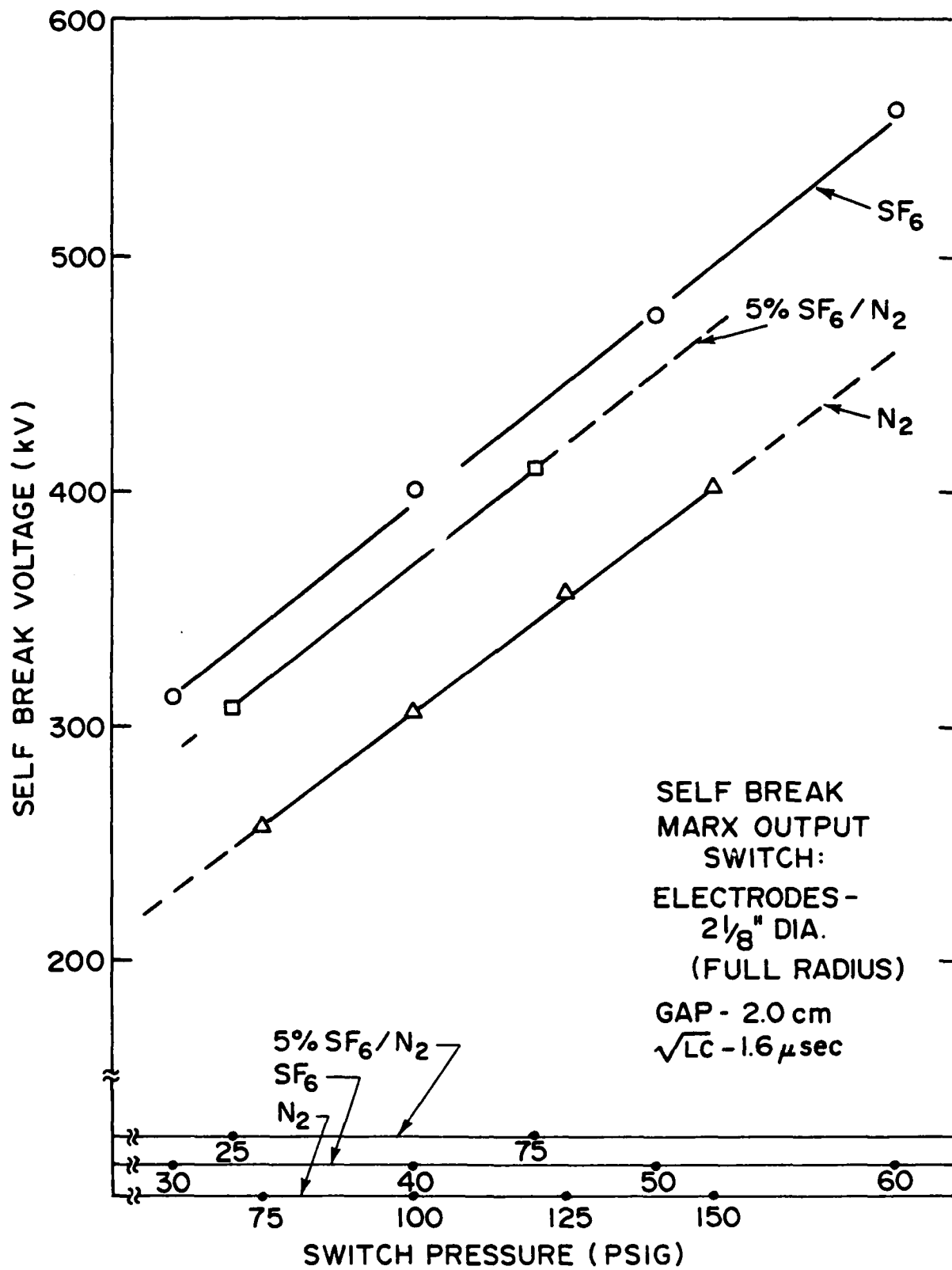


Fig. 4. Plot of self-breakdown voltage of the Marx output switch (S-2 in Fig. 3) as a function of gas pressure for three gases.

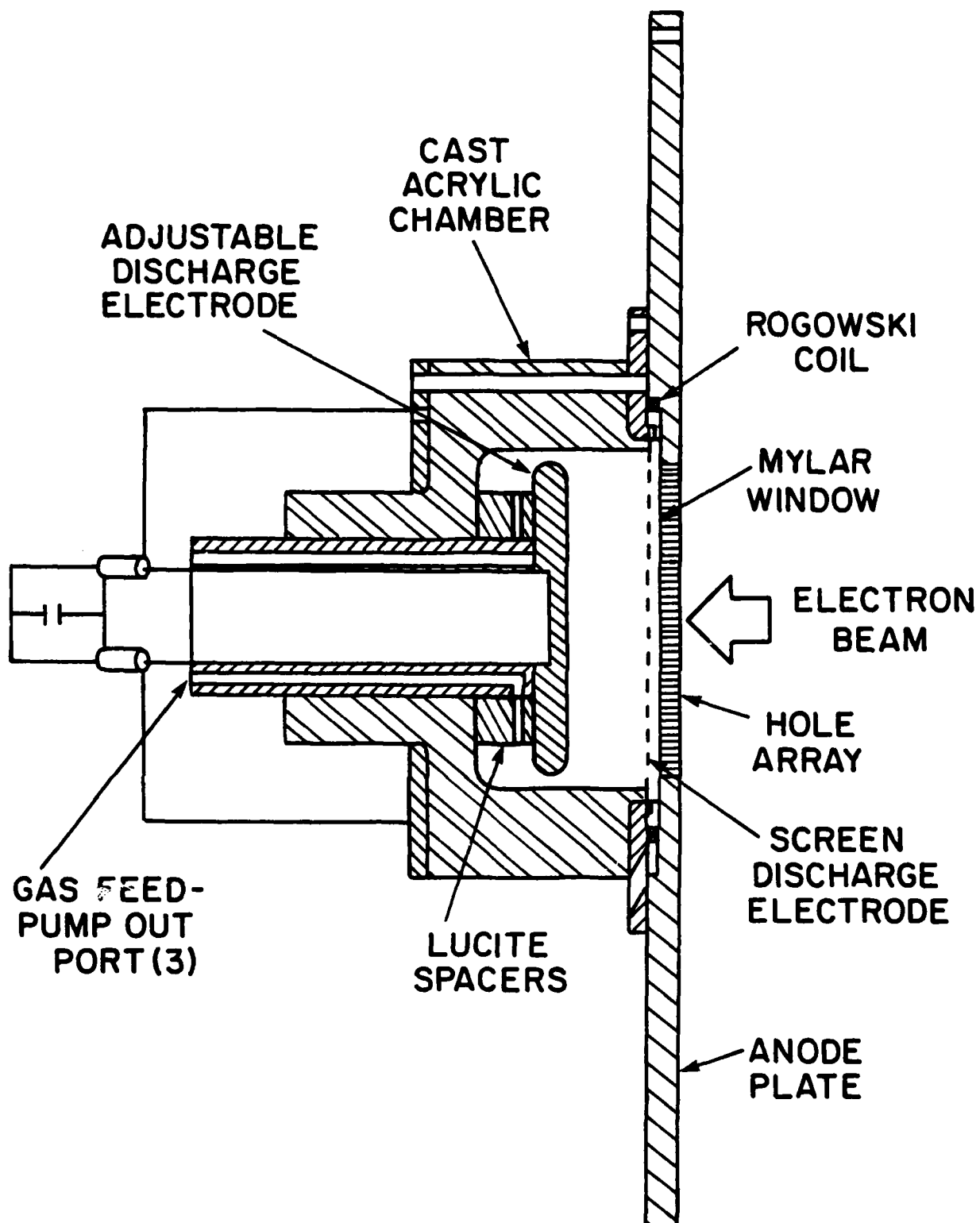


Fig. 13. Cross section of EBCS showing location of hardware and Rogowski loop for measuring  $I_b$ .

## B. Initial Results

An equivalent circuit for the switch/inductive store system is illustrated in Fig. 14. The circuit equation is

$$V_C(0) - \frac{1}{C} \int I dt - L \frac{dI}{dt} - I_{SW} R_{SW} = 0, \quad (1)$$

where  $C$  is the capacitance of the capacitor used as the current source,  $I = I_{SW} + I_b$  is the total current measured in the switch circuit,  $I_{SW}$  is the switch current,  $L$  is the value of the storage inductance,  $V_C(0)$  is the initial voltage across the capacitance  $C$ , and  $R_{SW}$  is the EBCS resistance. For all data shown here  $I \approx I_{SW}$ . Also, in all cases the switch polarity is such as to accelerate the injected e-beam electrons. The first two terms in Eq.(1) represent the instantaneous voltage across the capacitor,  $V_C$ . The third term is the voltage across the storage inductance. The voltage across the switch is  $V_{SW} = I_{SW} R_{SW}$ . By making  $R_{SW}$  large very quickly, large negative values of  $dI_{SW}/dt$  can be obtained, leading to high voltage across the switch. Because we are using an open circuit as a load, the output voltage  $V_0 = V_{SW}$ .

Results using a 5-atm mixture of 99% methane ( $\text{CH}_4$ ) as a base gas and 1% hexafluoroethane ( $\text{C}_2\text{F}_6$ ) as an attenuator in a switch of area  $A = 500 \text{ cm}^2$  and electrode separation  $\ell = 2 \text{ cm}$  with an e-beam  $AK = 7.8 \text{ cm}$  are shown in Fig. 15. In this figure the switch voltage,  $V_{SW}$  [determined from the measured  $I_{SW}$  and Eq. (1)], along with  $I_{SW}$  and  $I_b$  are plotted as a function of time. Also indicated is the initial charging voltage  $V_C(0) \approx 26 \text{ kV}$  on the capacitor  $C = 1 \mu\text{F}$ . For this shot the Marx charging voltage was  $V_m(0) = 35 \text{ kV}$  giving a peak e-beam energy of 210 keV. The storage inductance was  $L \approx 1.5 \mu\text{H}$ .

For these conditions, the ratio of the peak switch current to peak e-beam

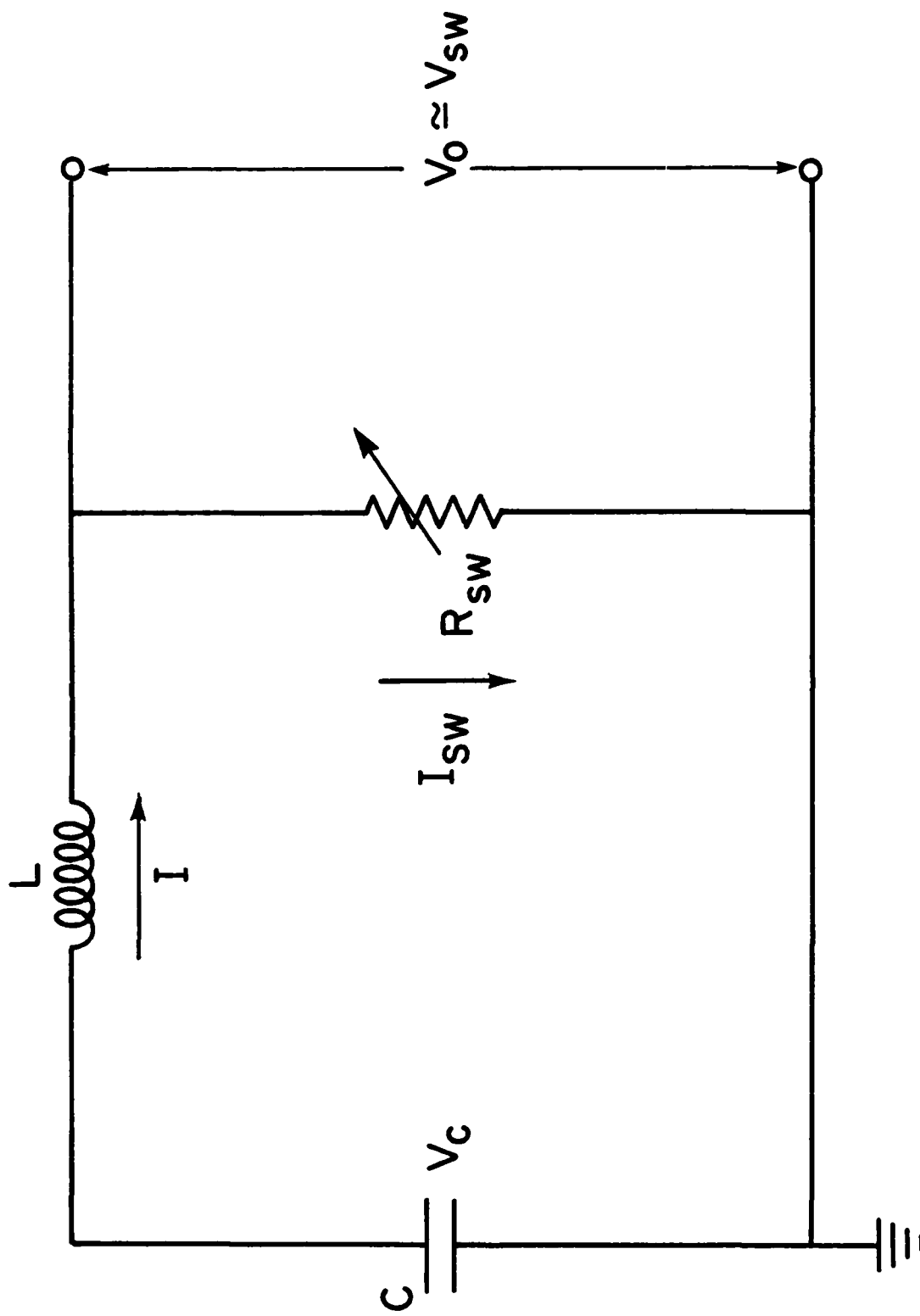


Fig. 14. Equivalent circuit of the inductive store system using the EBCS as the opening switch.

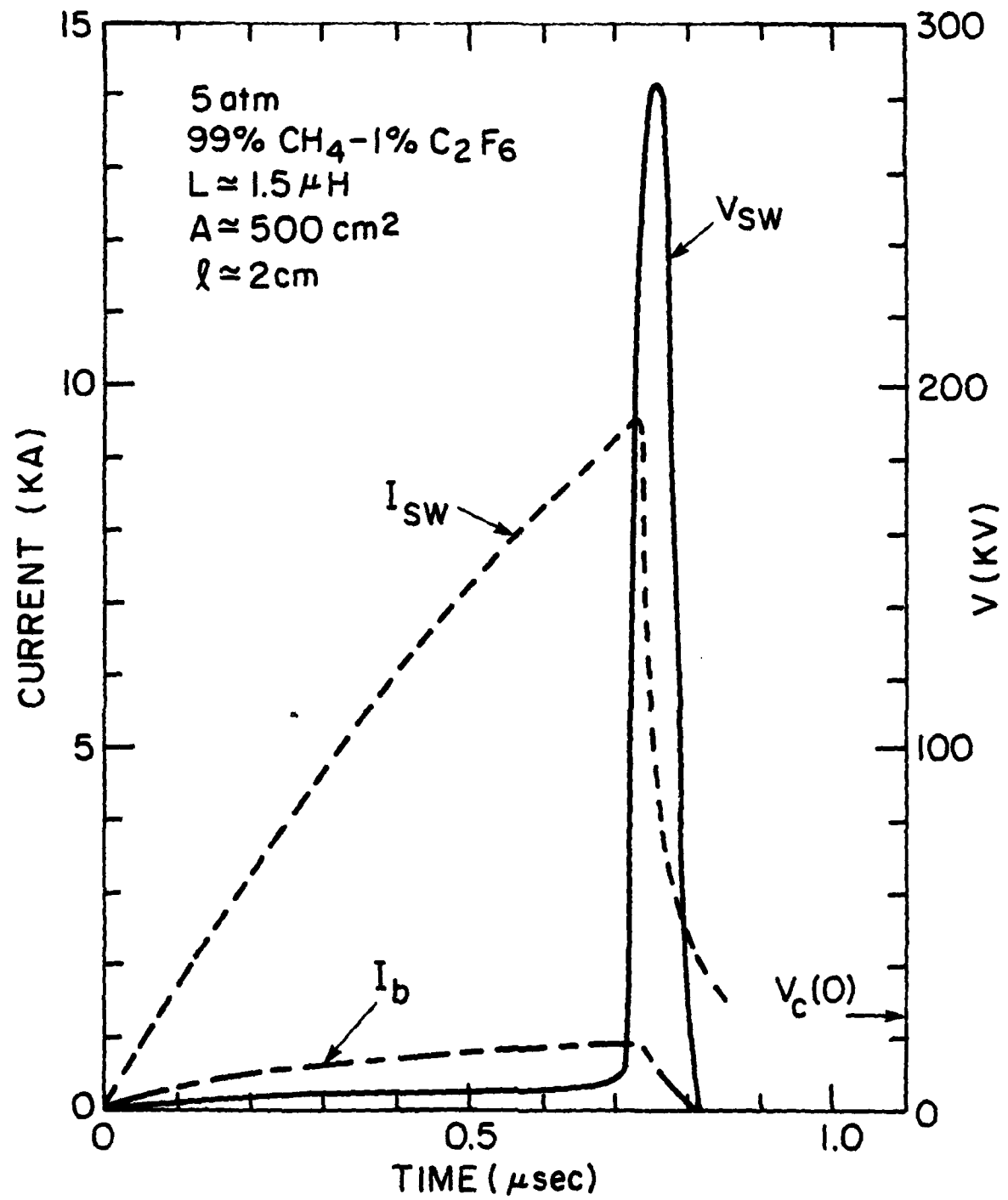


Fig. 15. Initial results from single pulse EBCS operation.

current, or current gain, was  $\epsilon \approx 10$ , the peak switch current density was  $= 20 \text{ A/cm}^2$ , and the peak voltage generated was  $V_{SW}^0 \approx 280 \text{ kV}$ . Thus we have obtained a voltage gain of  $V_{SW}^0/V_C(0) \approx 10$  with a similar pulse compression ratio (time to energize inductor/FWHM of output pulse). These parameters are well within a factor of two of the simple analytic predictions.<sup>1</sup> Note that the switch area is fairly uncertain because of e-beam profile effects. The peak switch current is only  $\approx 10 \text{ kA}$  because the divert switch on the Marx was triggered too early. The quarter period of the inductive store circuit ( $L = 1.5 \mu\text{H}$ ,  $C = 1.0 \mu\text{F}$ ) is  $\approx 2 \mu\text{s}$ , while the conduction phase lasts only  $\approx 0.7 \mu\text{s}$ . The maximum switch resistance was computed using Eq. (1) and is  $\approx 0.7 \Omega$ , which is comparable with  $\sqrt{L/C} \approx 1.2 \Omega$ . Note that  $R_{SW}$  could be smaller if the switch were to conduct longer.

In summary, the switch worked as predicted from the analytic analysis. A voltage pulse of approximately 280-kV amplitude and 60-ns FWHM was generated against an open circuit load. The voltage amplification factor and pulse compression ratio were both  $\approx 10$ . The results illustrated in Fig. 15 are from the first shots. No attempt was made either to optimize this data or make systematic variations in the parameters because of insufficient funds to continue the work.

#### V. Proposal for Future Work

Future work in the area of EBCS should concentrate on three main areas:  
1) switch gas optimization, 2) load considerations, and 3) repetitive operation.

In the first area, the effects of using attaching gases as well as behavior of the base gas must be quantitatively understood so that a low switch resistance during conduction together with a fast opening can be

obtained. That is, in principle, some gas or gas combination exists for which current gains of  $\epsilon = 10^2-10^3$  ( $10-10^2$  times higher than demonstrated in this work) are possible at e-beam currents of  $I_b \approx 1$  kA and with the same rapid recovery demonstrated in Fig. 15. This would require careful and systematic parameter variation with comparisons to calculations. The experiments should be done with a  $\geq 1 \mu s$  single pulse experiment to avoid complexity. In this and longer conduction time regimes both macroscopic breakdown and microscopic discharge stability should be investigated, as well as effects of gas decomposition.

The second area of work would determine how efficiently an inductive system employing an EBCS can be made to work. Again, this could be done in a single pulse mode, possibly at higher currents ( $\geq 100$  kA), and with a variety of relevant loads (e.g., e-beam diode or imploding plasma). This would also require developing an appropriate e-beam source.

Finally one should consider how a repetitive system could be designed. In general, repetitive inductive store systems have not been considered in detail within the context of a given problem, although some elementary analyses utilizing the EBCS have been performed.<sup>7,14</sup> This is an area that must be addressed (if for no other reason than) to identify potential problem areas.

#### Acknowledgments

The authors wish to express their gratitude to J.D. Shipman, Jr. for his assistance with the field plotting code and to J.M. Cameron and H. Hall for their expert technical assistance in the design, fabrication, and operation of the experiment. This work was supported by Naval Sea Systems Command, Office of Naval Research, and the Naval Surface Weapons Center, Dahlgren, VA.

## References

1. R.J. Commissio, R.F. Fernsler, V.E. Scherrer, and I.M. Vitkovitsky, Rev. Sci. Instrum. 55, 1834 (1984); and references therein.
2. V.E. Scherrer, R.J. Commissio, R.F. Fernsler, and I.M. Vitkovitsky, "Gaseous Dielectrics IV," L.G. Christophorou and M.O. Pace, Eds., Pergamon Press, NY (1984), p. 238; K. Schoenbach, G. Schaefer, M. Kristiansen, H. Kromphotz, H. Harjes, and D. Skaggs, *ibid*, p. 246.
3. G. Schaefer, K.H. Schoenbach, H. Krompholz, and M. Kristiansen, Laser and Particle Beams 2, 273 (1984).
4. R.J. Commissio, R.F. Fernsler, V.E. Scherrer, and I.M. Vitkovitsky, IEEE Trans. Plasma Sci. PS-10, 241 (1982); and references therein.
5. L.E. Kline, IEEE Trans. Plasma Sci. PS-10, 224 (1982).
6. M.R. Hallada, P. Bletzinger, and W.F. Bailey, IEEE Trans. Plasma Sci. PS-10, 218 (1982).
7. R.F. Fernsler, D. Conte, and I.M. Vitkovitsky, IEEE Trans. Plasma Sci. PS-8, 176 (1980).
8. R.J. Commissio, R.F. Fernsler, V.E. Scherrer and I.M. Vitkovitsky, Proceedings of the 4th IEEE Pulsed Power Conference, Albuquerque, NM (1983), IEEE Cat. No. 83CH1908-3, p. 87.
9. J.F. Lowry, L.E. Kline, and J.V.R. Heberlein, Proceedings of the 4th IEEE Pulsed Power Conference, Albuquerque, NM (1983), IEEE Cat. No. 83 CH1908-3, p. 94.; P. Bletzinger, *ibid.*, p. 37.
10. D.D. Hinshelwood, NRL Memo Report 5185, November 1983.
11. J.K. Burton, W.R. Glock, W.L. Lupton, Symposium on Engineering Problems of Fusion, Los Alamos Report LA-4250 (1969), p. DI-3-P.
12. J.D. Shipman, Jr., personal communication (1984).
13. G.F. Erickson, P.N. Mace, Rev. Sci. Instrum. 54, 586 (1983).
14. R.J. Commissio, R.F. Fernsler, V.E. Scherrer, and I.M. Vitkovitsky, NRL Memo Report 4975 (1982). ADA124312

**END**

**FILMED**

**11-85**

**DTIC**